Effect of a streamwise oscillating cylinder on a downstream cylinder wake

by

S. J. Xu and Y. Zhou*

Department of Mechanical Engineering

The Hong Kong Polytechnic University

Hung Hom, Kowloon, Hong Kong

*E-Mail: mmyzhou@polyu.edu.hk

ABSTRACT

Interference is experimentally investigated between a streamwise oscillating cylinder wake and that of a downstream stationary cylinder of identical diameter *d*. The flow was visualised using a laser illuminated fluorescence technique. The upstream cylinder was forced to oscillate harmonically in time at the amplitude of A/d = 0.5-0.67 and the frequency ratio, f_e/f_s = 0 ~ 2.0, where f_e is the cylinder oscillation frequency and f_s is the shedding frequency of vortices from an isolated stationary cylinder. At these experimental conditions, the shedding frequency of vortices from the oscillating cylinder locked on with the oscillation. It has been found that the flow structure (vortex pattern) varies with f_e/f_s and is virtually independent of the cylinder centre-to-centre spacing, L/d, at least for the L/d range presently investigated. Three flow regimes have been identified between f_e/f_s = 0 and 2. At $f_e/f_s < 0.8$, the shedding of vortices from the upstream oscillating cylinder is symmetrical, while that from the downstream stationary cylinder is anti-symmetrical. For $0.8 < f_e/f_s < f^*_c$ (≈ 1.35 ~ 1.4), where f^*_c is a critical frequency ratio, which may vary slightly with the oscillation amplitude A/d and the Reynolds number *Re*, vortices are shed alternately from either cylinder and wonder wildly in the lateral direction. As f_e/f_s exceeds f^*_c, the symmetrical and the anti-symmetrical shedding of vortices resume for the upstream and downstream cylinders, respectively. But the details of the flow structure are quite different from those at $f_e/f_s < 0.8$. For example, the binary structure, each consisting of a pair of counter-rotating vortices, is generated by the oscillating cylinder for $f_e/f_s > f^*_c$, but not for $f_e/f_s < 0.8$. The qualitative flow structure is further examined along with the quantitative data obtained using the particle image velocimetry and hot-wire techniques.

1. INTRODUCTION

Flow behind multiple structures is frequently seen in engineering. Examples include heat exchangers, offshore structures, power transmission lines and high-rise buildings. When the Reynolds number, *Re*, exceeds a critical value, the boundary layer will separate from a structure in a flip-flop manner. The alternate flow separation from the structure in turn produces a fluid excitation force, which may induce a structural oscillation at a significant magnitude. This oscillation will influence the flow around downstream structures. From another point of view, the documentation of the possible influence on the downstream cylinder wake is important for flow-control problems, where the unsteady flow pattern around a structure needs to be altered, either cancelled, e.g., to suppress flow-induced vibration or reinforced such as for transport enhancement in heat transfer applications. It is therefore of both fundamental and practical interests to investigate how an oscillating cylinder alter a downstream cylinder wake.

The simplest case of the multiple structures is a two-cylinder system, which may have side-by-side, in-tandem or staggered arrangements. The structural oscillation can be transverse or streamwise, or a combination of both. Previous studies mostly focused on the transverse oscillation of a single or two cylinders (e.g. Bearman 1984; Griffin & Hall 1991; Williamson & Roshko 1988; Ongoren & Rockwell 1988a). This is perhaps because the lift force on a structure is in many cases, say in an isolated cylinder case, (Chen 1987) one order of magnitude larger than the drag force. Subsequently the lateral structural oscillation prevails against that in the streamwise direction. However, the drag force is also significant; it could even exceed the lift, in particular in the context of multiple cylinders.

There have been a number of investigations involving a streamwise oscillating cylinder in a cross flow. Griffin & Ramberg (1976) studied the vortex formation around an isolated cylinder, which oscillated at small amplitude in the streamwise direction, at the onset of 'lock-on'. Here, lock-on refers to the situation where the vortex shedding frequency coincides with that of structural oscillation. Tanida et al. (1973) measured the lift and drag forces on two tandem circular cylinders, where the downstream cylinder oscillated longitudinally. They found that at Re = 4000 synchronization occurred when the shedding frequency of vortices from the downstream cylinder was half the oscillating frequency. Ongoren & Rockwell (1988b) investigated the flow patterns behind a cylinder oscillating in the streamwise direction at the oscillation amplitude A/d = 0.13 and the frequency ratio f_e/f_s = 0.5 ~ 4.0, where f_e is the oscillation or excitation frequency of the downstream cylinder and f_s is the vortex shedding frequency of an isolated stationary cylinder. This study complemented Tanida *et al.*'s measurement of unsteady loading on the cylinders. Two basic modes of vortex formation were identified, i.e. the symmetrical (in-phase) and the anti-symmetrical (out of phase) vortex formation from either side of the cylinder. Li et al. (1992) conducted a direct numerical simulation (DNS) of a streamwise oscillating cylinder in the wake of an upstream cylinder. They identified two flow regimes. In the 'vortex formation regime' at large cylinder-to-cylinder centre spacing L/d (L is defined in the absence of oscillation), vortex streets developed behind both cylinders. The street generated by the upstream cylinder was important compared to the forced oscillation and dominated the flow, resulting in a very small zone of synchronization. In the 'vortex suppression regime' at small L/d, this street became weak and had little effect on the downstream cylinder wake. Recently, Cetiner & Rockwell (2001) studied the lock-on state of a streamwise oscillating cylinder in a cross flow (f_e/f_s = 0.5 ~ 3.0). It was found that the time-dependent transverse force was phase-locked to the cylinder motion and the vortex system occurred both upstream and downstream of the cylinder. However, how a streamwise oscillating cylinder would affect a downstream cylinder wake has not been investigated. Many questions may be asked. How do the wakes of two tandem cylinders, one vibrating and one stationary, interact? What is the dominant flow structure when the upstream oscillating cylinder is locked on with the vortex shedding? In this paper, the flow structure refers to the vortex pattern. Also, how would the flow structure change in the absence of locking-on phenomenon? These issues are interesting and motivate the present investigation.

The present work aims to investigate the effect of a streamwise oscillating cylinder on a downstream cylinder wake. The investigation employs a laser-illuminated fluorescence (LIF) technique to visualise the flow structures behind the oscillating cylinder and the downstream stationary cylinder. The qualitative flow images are examined along with the quantitative flow field as obtained using the particle image velocimetry (PIV).

2. EXPERIMENTAL DETAILS

2-1 Laser-illuminated flow visualization in a water tunnel

The LIF measurements were carried out in a water tunnel, which has a square working section (0.15m × 0.15m) of 0.5m long. The working section is made up of four 0.02m thick perspex panels. A regulator valve controls the flow speed and the maximum velocity attained in the working section is about 0.32m/s. Further details of the water tunnel can be found in Zhou *et al*. (2001).

Two acrylic circular tubes of an identical diameter d = 0.01 m were horizontally mounted in tandem at the mid-plane of the working section. They were cantilever-supported; the gap between the cylinder tip and the working

section wall was about 0.5 mm, thus resulting in a blockage of about 7%. The upstream cylinder, driven by a D.C. motor through a linkage system, oscillated harmonically in time in the streamwise direction. The D. C. motor was controlled by a microcomputer so that the oscillating frequency of the cylinder could be precisely obtained. The structural oscillation amplitude was fixed at A/d = 0.5, while f_e was varied so that f_e / f_s ranged from 0 to 2. The first-mode natural frequency of the fluid-cylinder system was estimated to be about 32 Hz, one order of magnitude greater than the maximum f_e (= 2 Hz), that is, the imposed oscillation was far away from resonance.

Dye (Rhodamine 6G 99%), which has a faint red colour and will become metallic green when excited by laser, was introduced through one injection pinhole located at the mid-span of the cylinder at 90°, clockwise and anti-clockwise, respectively, from the leading stagnation point. A thin laser sheet, which was generated by laser beam sweeping, provided illumination vertically over $0 \le x/d \le 10$ at the mid-plane of the working section. A Spectra-Physics Stabilite 2017 Argon Ion laser with a maximum power output of 4 watts was used to generate the laser beam and a professional digital video camcorder (JVC GY-DV500E), set perpendicular to the laser sheet, was used to record the dye-marked vortex streets at a framing rate of 25 frames per second.

Measurements were carried out for L/d = 2.5**,** 3.5 and 4.5 and Re ($\equiv \dfrac{U_\infty d}{\nu}$) = 150, 300, 600 and 1000, where U_∞ is the free-stream velocity and ν is the kinematic viscosity.

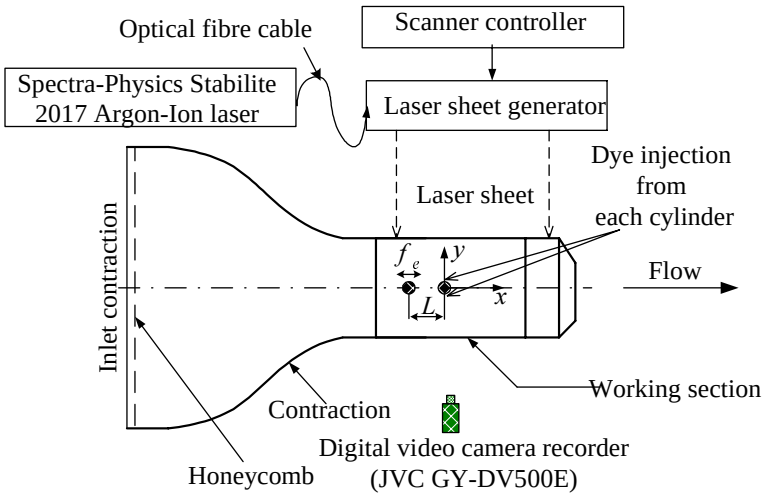

Figure 1 Experimental set-up for flow visualization in a water tunnel.

2-2 Wind tunnel experiments

Wind tunnel The PIV measurement was carried out in a closed-loop wind tunnel to obtain both qualitative and quantitative data at a range of f_e/f_s. The wind tunnel has a square working section (0.6m x 0.6m) of 2.4m in length. The view window of the working section was made of optic glass in order to maximize the signal-to-noise ratio in PIV measurements. The wind speed in the working section can be adjusted from about 0.3m/s to 50m/s.

Cylinder Assembly The cylinder assembly was designed similarly to that used for the LIF measurements in the water tunnel. Two aluminium alloy cylinders of an identical diameter of 0.015 m were cantilever-supported in the horizontal mid-plane of the working section. The length of both cylinders inside the tunnel was 0.35 m, thus resulting in a blockage of 1.25% and an aspect ratio of about 23. A 0.15 m long section from the free end of each cylinder was replaced by a transparent acrylic tube in order to allow the laser sheet to shine through, thus minimizing the shadow effects in the PIV measurement. One microcomputer-controlled DC motor system was used to drive the upstream cylinder to oscillate. The oscillation amplitude varied from A/d = 0.5 to 0.67, and f_e/f_s ranged from 0 to a maximum of 1.42. The first-mode natural frequency of each cylinder was about 272 Hz, which is a factor of 12 times the maximum f_e (= 22Hz). To minimize the reflection noise generated by the laser sheet shining on the cylinders, the surface of both cylinders were painted black except a 20 mm long section at 0.12 m from the free end on the acrylic section. In the free-stream, the longitudinal turbulence intensity was measured to be approximately 0.4%.

PIV measurements The velocity field was measured using a Dantec standard PIV2100 system for $P / d = 3.5$ and $Re = 1150$. The f_e / f_s ratio investigated ranged from 0 to 1.8. Flow was seeded by smoke, which was generated from Paraffin oil, of a particle size around 1 μm in diameter. Flow was illuminated in the plane of mean shear by two NewWave standard pulsed laser sources of a wavelength of 532nm, each having a maximum energy output of 120 mJ. Digital particle images were taken using one CCD camera (HiSense type 13, gain × 4, double frames, 1280×1024 pixels). A Dantec FlowMap Processor (PIV2100 type) was used to synchronize image-taking and illumination**.** Each image covered an area of 115 mm × 92 mm of the flow field, i.e. $x / d = -4.3$ $d \sim 4.3$ d and $y / d = -3.1$ $d \sim 3.1d$; the x and y coordinates and their origin are defined in Figure 1b. The longitudinal and lateral image magnifications were identical, i.e. 0.09mm/pixel. Each laser pulse lasted for 0.01μ*s*. The interval between two successive pulses was typically 50μ*s*. Thus, a particle would only travel 0.05mm (0.56 pixels or 0.003 *d*) at $U_\infty = 1.0$ *m*/*s*. An optical filter was used to allow only the green wavelength (532nm) generated by laser to pass.

Since both cylinders were included in the PIV images, which could cause errors in deriving velocities around the cylinders, they were masked using a built-in masking function in the Dantec PIV2001 system before calculation of particle velocities. In the image processing, 32 x 32 rectangular interrogation areas were used. Each interrogation area included 32 pixels (≈ 0.2 *d*) with 50% overlap with other areas in both the longitudinal and lateral directions. The ensuing in-plane velocity vector field consisted of 79 × 63 vectors, which gave the same number of spanwise vorticity component, ω_z, which may be approximately obtained based on particle velocities. The spatial resolution for vorticity estimate was about 1.43 mm or 0.095*d*.

3. RESULTS AND DISCUSSION

The behaviours of the wake of an isolated oscillating cylinder may depend on the combination of A/d and f_e/f_s (Karniadakis & Triantafyllou 1989). When the oscillating cylinder is placed upstream of a stationary cylinder, the parameter L/d is also important. A thorough understanding of this problem may further need to understand the effect of *Re*. Our preliminary experiments indicated that over the range of $L/d = 2.5$ and 4.5 presently investigated the dependence of the flow structure on L/d is relatively weak, compared with the case of two stationary cylinders. So is that on *Re*. But the flow structure may vary drastically with a different combination of A/d and f_e/f_s, resembling the case of an isolated streamwise oscillating cylinder. This is perhaps because the oscillating wake generated by the upstream cylinder could dominate for $L/d \leq 4.5$. The present investigation will largely focus on the effect of f_e/f_s on the flow structure due to a limitation on pages. For the range of $0 < f_e/f_s \leq 2$ and $A/d = 0.5 \sim 0.67$, vortex shedding occurs for both cylinders. Furthermore, the lock-on state, that is, the shedding frequency f_{su} of vortices from the upstream cylinder is coincident with f_e, occurs irrespective of the f_e/f_s value. Three flow regimes have been identified based on the flow structure behind the downstream stationary cylinder, each showing a completely distinct behaviour.

3-1 Symmetric-staggered binary street regime

For $1.6 < f_e/f_s \leq 2$ and a fixed $A/d = 0.5$, the flow behind the downstream cylinder is characterised by a binary street that consists of two outer rows (close to the free-stream) of symmetrically arranged vortices originated from the upstream oscillating cylinder and two inner rows (near the centreline) of anti-symmetrically arranged vortices generated by the downstream stationary cylinder. The downstream cylinder sheds vortices alternately, while the upstream one sheds symmetrically. This is evident in photographs (Figure 2) obtained from the LIF measurement in the water tunnel ($f_e/f_s = 1.8$, $A/d = 0.5$ and $Re = 300$).

Note that each structure shed from the upstream cylinder embraces a pair of counter-rotating vortices. We may refer to this structure as a binary vortex. In order to understand the formation of this pair of vortices, sequential photographs of various phases in one typical cycle of the cylinder oscillation (Figure 2) are examined. The phase of each photo is indicated in Figure 2i, where t and X represent time and the streamwise displacement from the reference position ($X = 0$) of the upstream cylinder, respectively. The vertical line near the upstream cylinder marks the reference position. When the upstream cylinder moves oppositely to the flow direction (Figures 2a – 2c), one clockwise rotating vortex A_{u1} above the centreline forms due to vortex shedding. As the cylinder moves from $-A$ to $+A$ in the same direction as the flow (Figures 2c – 2f), the fluid near the cylinder wall moves along with the cylinder under the viscosity effect, but the fluid further away now moves oppositely (right to left) relative to the cylinder. The average moving velocity of the cylinder is about 3.38 cm/s ($f_e = 1.2$ Hz), while that of water was 2.7 cm/s. Thus, the maximum velocity of water relative to the cylinder is estimated to be about 1.07 cm/s, resulting in an instantaneous Reynolds number (based on this relative velocity and cylinder diameter) of 120, which exceeds the critical Reynolds number (≈ 40, e.g. Schlichting & Gersten 2000) for vortex shedding. Therefore, a vortex, A_{u2}, of the anti-clockwise sense begins to form. Eventually, the structure containing a pair of counter-rotating vortices A_{u1} and A_{u2} separates from the cylinder (Figures 2f-h) and evolves downstream.

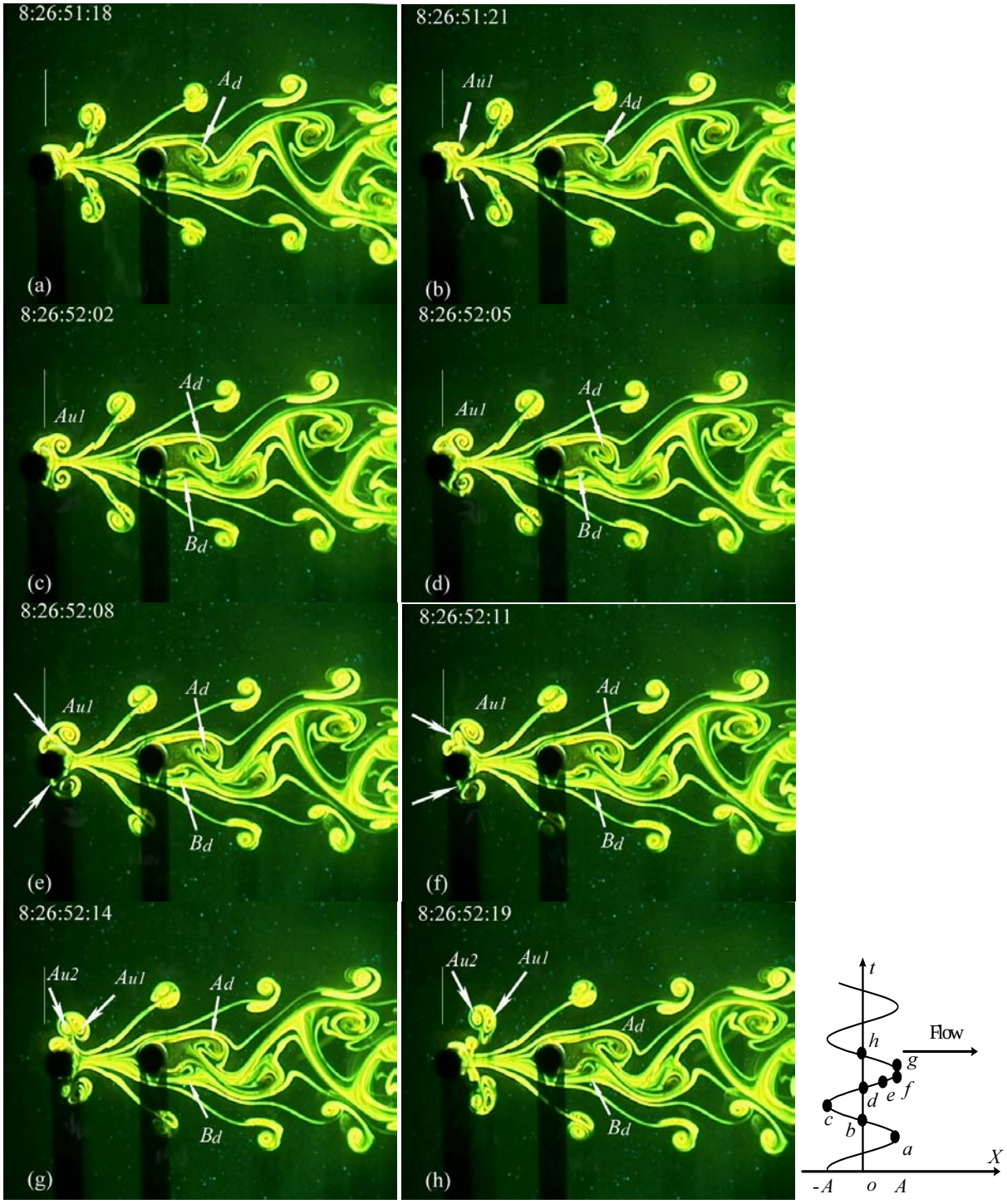

Figure 2 Sequential photographs of a symmetric-staggered binary street at f_e/f_s = 1.8. L/d = 3.5, Re = 300, A/d = 0.5.

The PIV measurement may provide quantitative as well as qualitative information. The maximum f_e/f_s achievable for the present experimental set-up was 1.42 in the wind tunnel. In order to obtain the symmetric and staggered binary street at this f_e/f_s, A/d was increased to 0.67. Figure 3 presents two typical plots of the contours of spanwise vorticity $\omega_z^* = \omega_z d / U_\infty$ obtained from the PIV measurement (L/d = 3.5, A/d = 0.67, Re = 1150, f_e/f_s = 1.42). Vortices generated by the downstream cylinder exhibit a spatially staggered arrangement, consistent with the LIF measurement (Figure 2). The binary vortices or counter-rotating vortex pairs near the upstream cylinder are evident in both plots and are identifiable beyond the downstream cylinder. These vortices are formed symmetrically about the flow centreline and remain so as they move downstream. The negative vorticity concentration, corresponding to the vortex A_{u1} in Figure 2, in the binary vortex above the flow centreline tends to have a greater strength than the positive concentration corresponding to A_{u2} in terms of size and the maximum

magnitude of ω_z^*. The observation supports the earlier interpretation on the formation process of A_{u1} and A_{u2} based on sequential photographs (Figure 2). When the cylinder moves oppositely to the flow to form A_{u1}, the velocity gradient in the shear layer is expected to increase, thus generating the vortex of a larger strength. The maximum magnitude of ω_z^* of the binary vortex is about 9, significantly larger than that (< 4) shed from the downstream cylinder. Two factors could be responsible. Firstly, the lock-on condition may enhance the binary vortex strength. Secondly, the upstream cylinder movement opposite to the flow increases the velocity gradient of the shear layer and subsequently the vorticity concentration of the binary vortices. The binary vortex is characterised by a very fast decay, its maximum magnitude of ω_z^* dropping from 7 ~ 9 near the upstream cylinder to about 3 when reaching the downstream cylinder. This is probably because of cancellation between the positive and negative vorticity concentrations within the binary vortex.

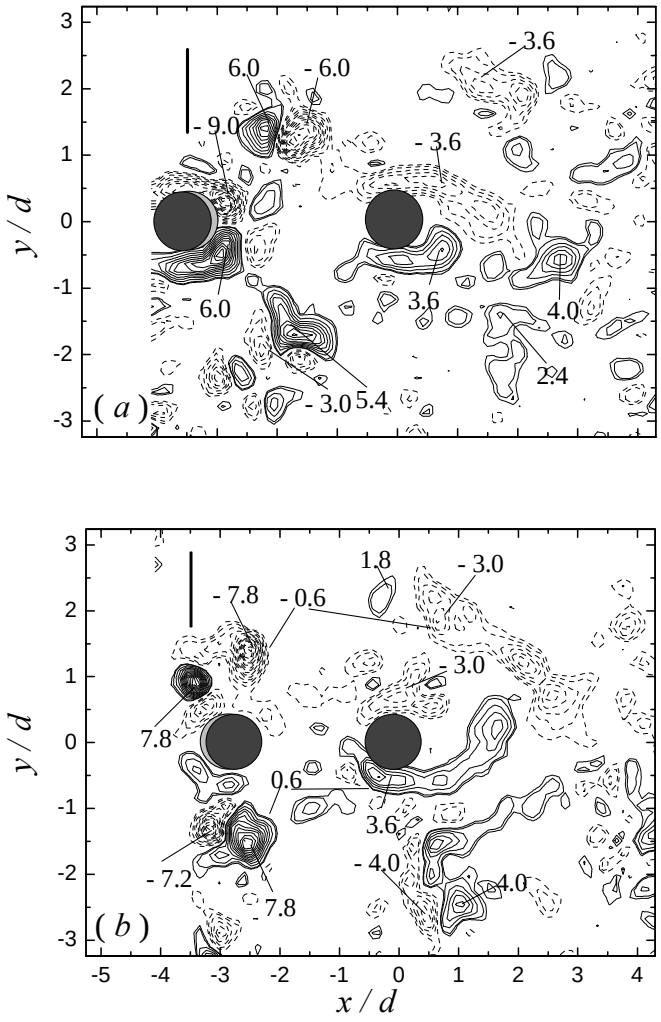

Figure 3 Instantaneous vorticity contours $\omega^* = \omega d / U_\infty$ obtained from the PIV measurement (the contour increment = 0.6, A/d = 0.67, Re = 1150, L/d = 3.5. f_e/f_s = 1.42).

3-2 Staggered binary street regime

As f_e/f_s reduces to 0.8 ~ 1.6 at A/d = 0.67, the flow structure experiences a dramatic change into a more complicated structure, as illustrated in Figure 4 for f_e/f_s = 1.08. A careful examination reveals that the flow behind the downstream stationary cylinder consists of two outer rows of binary vortices such as A_u and B_u, originated from the upstream cylinder, and two inner rows of single vortices, denoted by A_d and B_d, generated by the downstream cylinder. Alternate vortex shedding occurs for both cylinders. However, the two successive vortices alternately shed from the upstream cylinder quickly move to one side of the wake before reaching the downstream cylinder. For example, A_{u2} was shed from the upper side of the upstream cylinder but crossed the centreline to approach A_{u1} shed from the lower side of the same cylinder. The two vortices eventually paired to

form a binary vortex in the lower outer row of the binary street behind the downstream cylinder. The evolution of vortices B_{u1} and B_{u2}, which were shed from the upper and lower side of the upstream cylinders, respectively, is quite similar to that of A_{u1} and A_{u2}, though they end up with a binary vortex in the upper outer row of the binary street.

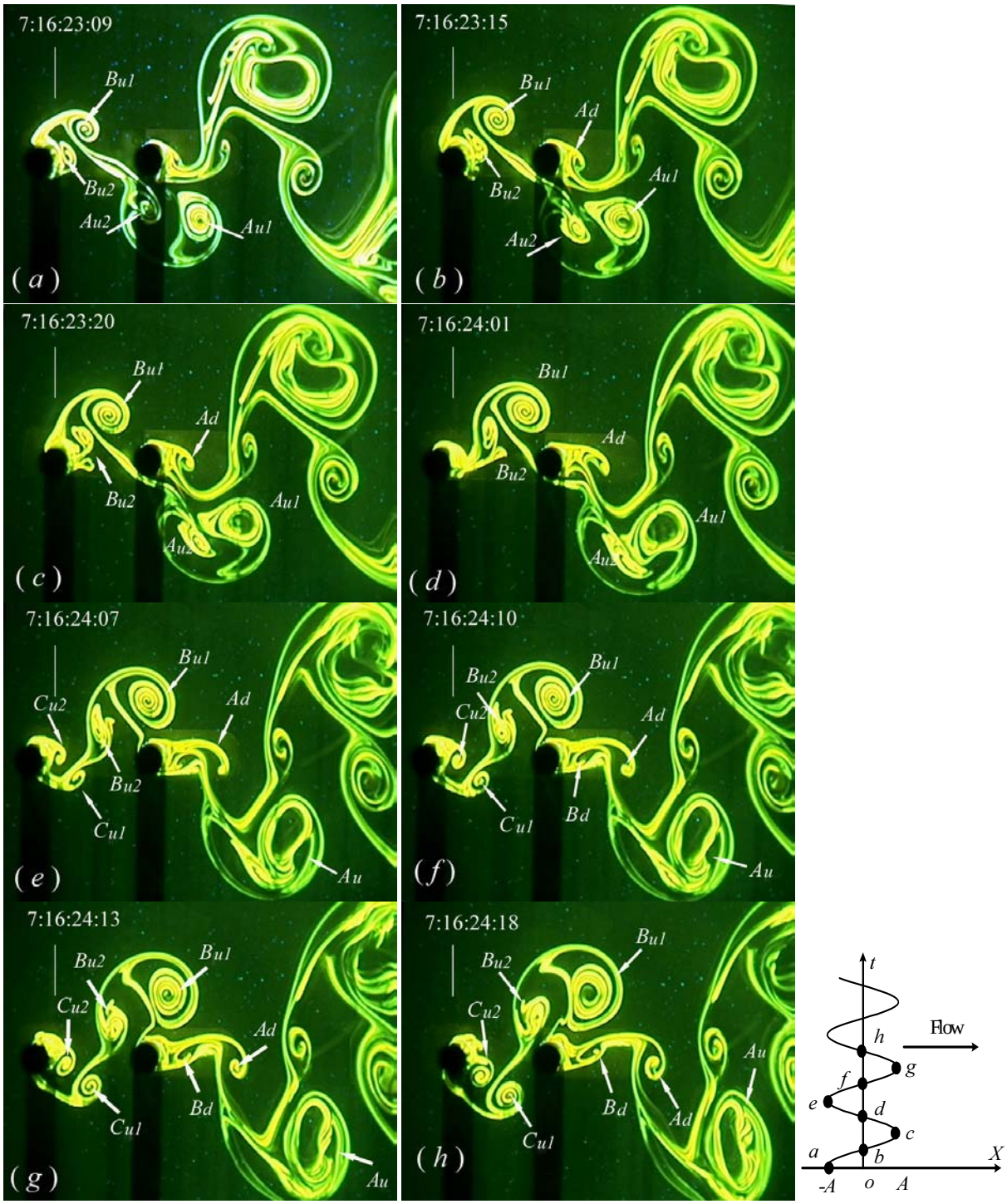

Figure 4 Sequential photographs of a staggered binary street at f_e/f_s = 1.08. L/d = 3.5, Re = 300, A/d = 0.5.

The upstream cylinder movement plays a key role to induce a vortex across the centreline merging with the vortex on the other side of the wake. Noting the vortex shedding frequency f_{su} is locked on to f_e. Each time when the cylinder moves oppositely, right to left, to the flow direction, one vortex begins to form and separate from the cylinder. This process is exemplified in Figures 4d – 4f, where the vortex C_{u1} is in its initial stage of formation. The cylinder movement opposite to the flow is likely to reduce the backpressure of the cylinder. The very low pressure in the base region draws in C_{u1} to cross the centreline. The ensuing cylinder movement in the flow direction (Figures 4g – 4h) may act to push C_{u1} further down.

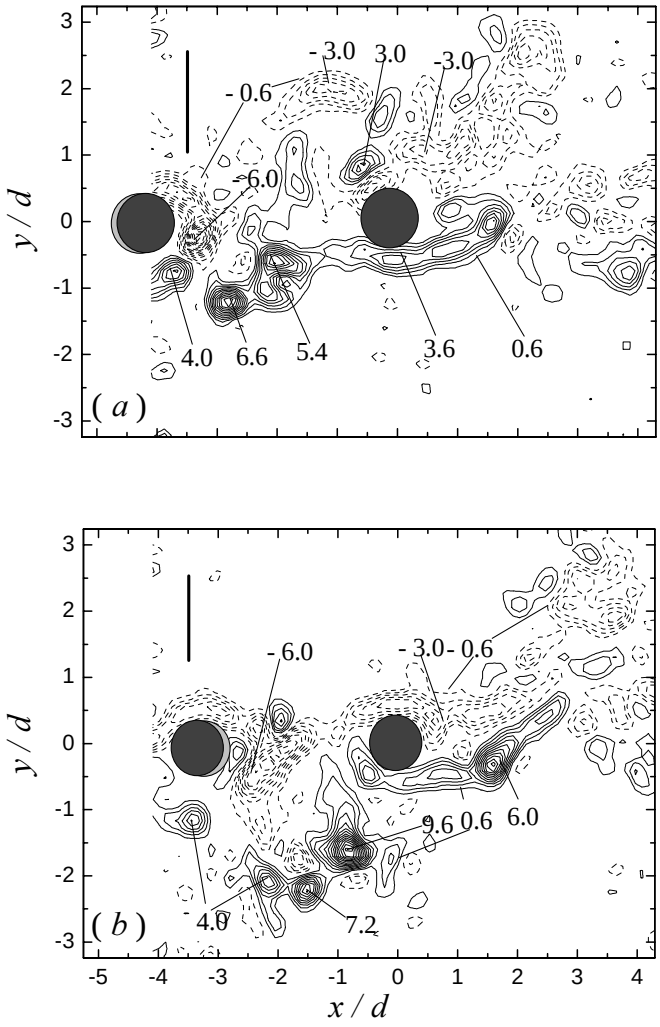

Figure 5 Instantaneous vorticity contours $\omega^* = \omega d/U_\infty$ obtained from the PIV measurement (the contour increment = 0.6, A/d = 0.67, Re = 1150, L/d = 3.5. $f_e/f_s = 0.85$).

The flow structure observed in the LIF photographs is identifiable in the ω_z^* contours obtained from the PIV measurement (Figure 5). In similarity to the symmetric and staggered binary street regime, vortices generated by the upstream oscillating cylinder are characterised by a higher vorticity concentration. Again, the vorticity concentration shed from the upstream cylinder decays quickly, probably because of vorticity cancellation between the two merged counter-rotating vortices such as A_{u1} and A_{u2}.

3-3 Single staggered street regime

The flow is characterised by a single staggered street for $0 < f_e/f_s \lesssim 0.8$. Figure 6 present representative sequential photographs at $f_e/f_s = 0.5$, $L/d = 3.5$, $A/d = 0.5$ and $Re = 150$ obtained from the LIF measurement. Under the influence of the downstream stationary cylinder, vortices A_u and B_u are separated alternately from the upper and lower sides, respectively, of the upstream cylinder. On reattaching the downstream cylinder, they separate, perhaps along with the shear layers around this cylinder, to form a staggered vortex street downstream. Apparently, the vortex shedding frequency of the downstream cylinder must be the same as that of the upstream cylinder.

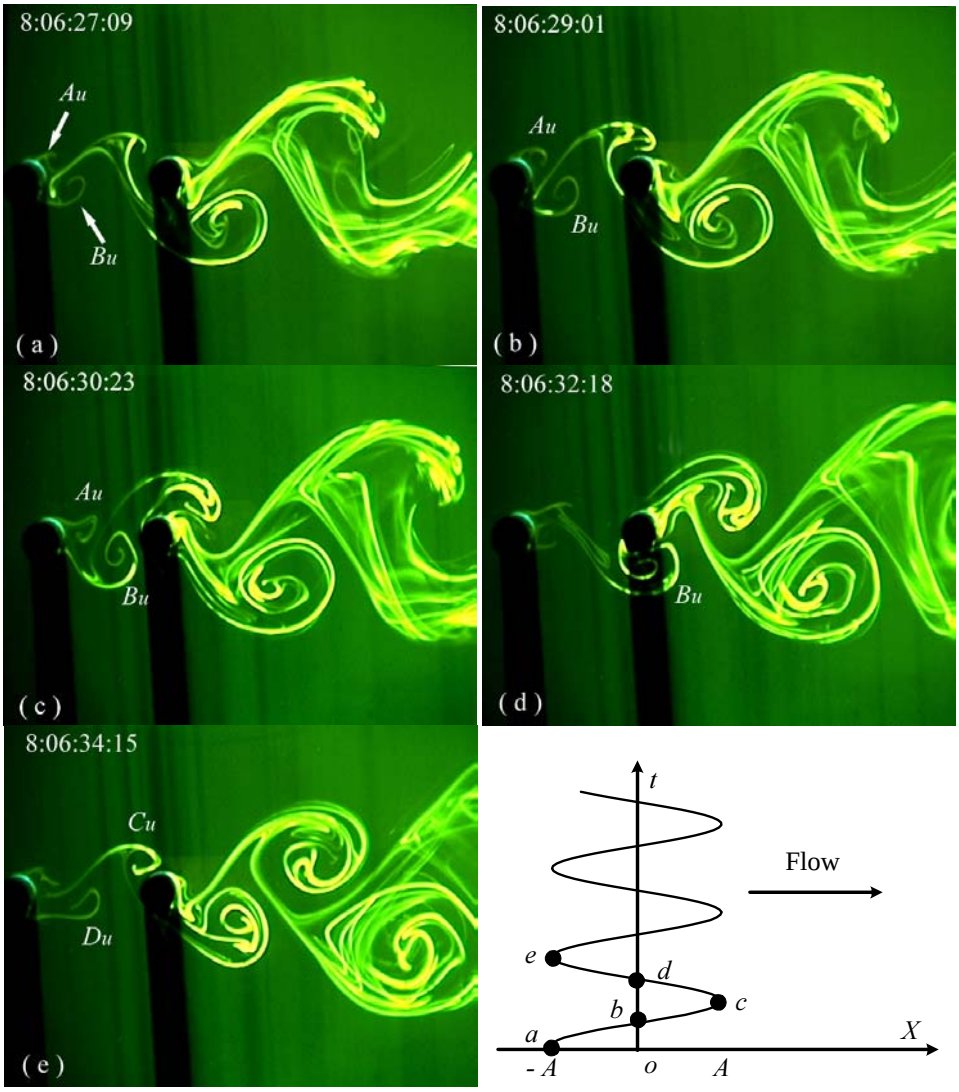

Figure 6 Photographs of a single staggered street at f_e/f_s = 0.5. L/d = 3.5, Re = 150, A/d = 0.5.

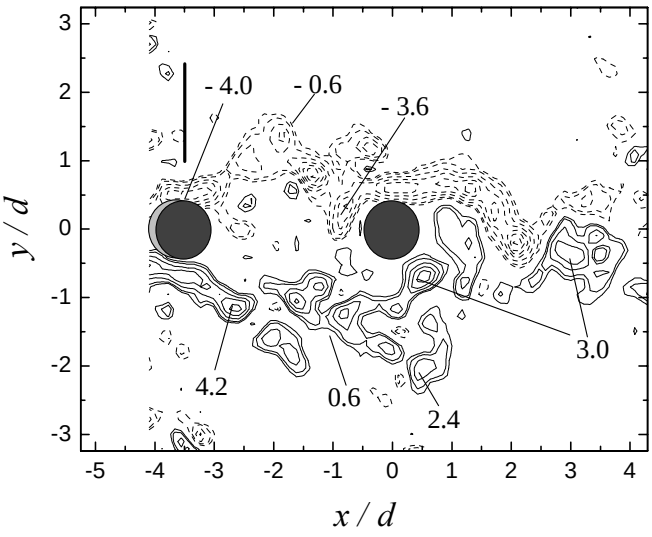

Figure 7 Instantaneous vorticity contours $\omega^* = \omega d/U_\infty$ obtained from the PIV measurement (the contour increment = 0.6, A/d = 0.67, Re = 1150, L/d = 3.5. f_e/f_s = 0.52).

The ω_z^* contours (Figure 7) obtained from the PIV measurement exhibit a flow structure similar to that observed in the LIF measurement. The vorticity concentration experiences a rapid decay as vortices are advected from the upstream to the downstream cylinder, the maximum magnitude of ω_z^* declining from about 4.2 to 2.4. The vorticity loss is probably caused by cancellation and interference between positive and negative vorticity in the base region, as in an isolated cylinder case (Cantwell 1983).

4. CONCLUSIONS

The effect of a streamwise oscillating cylinder on the downstream cylinder wake has been experimentally investigated using the LIF and PIV techniques. For a fixed A/d (= 0.5 ~ 0.67), the flow structure may vary dramatically with f_e/f_s. Three distinct flow regimes have been identified for $0 < f_e/f_s < 2$.

At f_e/f_s = 1.6 ~ 2, the downstream cylinder sheds vortices alternately, while the upstream one sheds symmetrically. A binary vortex street occurs behind the downstream cylinder, which consists of two outer rows of symmetrically arranged vortices originated from the upstream oscillating cylinder and two inner rows of staggered vortices generated by the downstream stationary cylinder. This flow structure may be referred to as the symmetric and staggered binary street regime.

For $0.8 \precsim f_e/f_s \precsim 1.6$, alternate vortex shedding occurs for both cylinders. The flow behind the downstream cylinder is characterised by a binary vortex street that consists of two outer rows of binary vortices, originated from the upstream cylinder, and two inner rows of single vortices shed by the downstream cylinder. The vortices in the two outer or two inner rows are spatially staggered, thus called the staggered binary street regime.

One single staggered street emerges behind the downstream cylinder at $f_e/f_s \precsim 0.8$.

ACKNOWLEDGEMENTS
The authors wish to acknowledge support given to him by the Research Grants Council of the Government of the HKSAR through Grants PolyU5125/98E..

REFERENCES

Bearman, P. W. 1984 Vortex sedding from oscillating bluff bodies. *Ann, Rev. Fluid Mech.* **16**, 195-222.

Cantwell, B. & Coles, D. 1983 An experimental study of entrainment and transport in the turbulent near wake of a circular cylinder. *J. Fluid Mech.* **136**, 321-374.

Cetiner, O. & Rockwell, D. 2001 Streamwise oscillations of a cylinder in a steady current (Part I, Locked-on states of vortex formation and loading; Part II, Free-surface effects on vortex formation and loading). *Journal of Fluid Mechanics*, **427**, pp1-59.

Chen, S. S. 1987 *Flow-induced Vibration of Circular Cylinder Structures*. Hemisphere Publishing Corporation. pp.260.

Duncan, W. J., Thom, A. S. and Young, A. D. 1967 The mechanics of fluids. The English language book society and Edward Arnold (publishers) Ltd. (England). pp124-127.

Griffin, O. M. and Hall, M. S. 1991 Review – vortex shedding locked-on and flow control in bluff-body wakes. *Trans. ASME: J. Fluids Engng*. 113, 526-537.

Griffin, O. M. and Ramberg, S. E. 1976 Vortex shedding from a cylinder vibrating in line with an incident uniform. *J. Fluid Mech.* **75**, 257-271.

Karniadakis, G E & Triantafyllou, G 1989 Frequency selection and asymptotic states in laminar wakes. *J. Fluid Mech.* **199**, 441-469.

Ongoren, A. and Rockwell, D. 1988a Flow structure from an oscillating cylinder. Part I. Mechanisms of phase shift and recovery in the near wake. *J. Fluid Mech*. **191**, 197-223.

Ongoren, A. and Rockwell, D. 1988b Flow structure from an oscillating cylinder. Part II. Mode competition in the near wake. *J. Fluid Mech*. **191**, 225-245.

Schlichting, H. and Gersten, K. 2000 *Boundary layer theory*. 8th revised and enlarge edition. Springer-Verlag Berlin Heidelberg, pp22.

Tanida, Y, Okajima, A & Watanabe Y 1973 Stability of a circular cylinder oscillating in a uniform flow or in a wake. *J. Fluid Mech.* **61**, 769-784.

Williamson, C. H. K. and Roshko, A. 1988 Vortex formation in the wake of an oscillating cylinder. *J. Fluids and Structures*. **2**, 355-381.

Zhou, Y., Wang, Z. J., So, R. M. C., Xu, S.J. and Jin, W. 2001 Free vibrations of two side-by-side cylinders in a cross flow, *Journal of Fluid Mechanics*, **443**, 197-229.